

SAPO-11을 이용한 억새와 Random Polypropylene의 촉매 열분해

강현구* · 유미진* · 박성훈** · 전종기*** · 김상채**** · 박영권*****†

*서울시립대학교 에너지환경시스템공학과, **순천대학교 환경공학과, ***공주대학교 화학공학과
****목포대학교 환경교육과, *****서울시립대학교 환경공학부

(2012년 12월 14일 접수, 2013년 1월 25일 수정, 2013년 1월 26일 채택)

Catalytic Pyrolysis of Miscanthus and Random Polypropylene over SAPO-11

Hyeon Koo Kang*, Mi Jin Yu*, Sung Hoon Park**, Jong-Ki Jeon***,
Sang-Chai Kim****, and Young-Kwon Park*****†

*Graduate School of Energy and Environ. System Eng., University of Seoul, Seoul 130-743, Korea

**Department of Environmental Engineering, Sunchon National University, Suncheon 540-950, Korea

***Department of Chemical Engineering, Kongju National University, Cheonan 331-717, Korea

****Department of Environmental Education, Mokpo National University, Muan, 534-729, Korea

*****School of Environmental Engineering, University of Seoul, Seoul 130-743, Korea

(Received December 14, 2012; Revised January 25, 2013; Accepted January 26, 2013)

초록: SAPO-11을 억새와 random polypropylene(random PP)의 촉매 열분해에 최초로 적용하였다. 열중량 분석 결과 SAPO-11은 억새의 탈수 반응을 촉진시키고, char의 생성을 억제하는 것으로 나타났다. Random PP의 열분해 결과, random PP의 분해온도와 활성화에너지는 촉매를 사용함에 따라 크게 감소하였다. 억새의 무촉매 열분해 반응에 의해 생성되는 oxygenate 생성물들 중에서 levoglucosan이 주 생성물이었다. SAPO-11 촉매 열분해 결과, 상당 부분의 levoglucosan이 furans, phenolics, aromatics 등의 부가가치가 큰 화합물로 전환하였다. 반면, random PP는 가솔린, 디젤 범위의 탄화수소를 생성하였다.

Abstract: SAPO-11 was applied for the first time to the catalytic pyrolysis of miscanthus and random polypropylene (random PP). Thermogravimetric analysis confirmed that SAPO-11 promoted the dehydration of miscanthus while suppressing the formation of char. In the pyrolysis of random PP, the decomposition temperature and activation energy were reduced by using a catalyst. A large fraction of levoglucosan, which was the main oxygenate product from the non-catalytic pyrolysis of miscanthus, was converted to high value-added products, such as furans, phenolics and aromatics using SAPO-34. The catalytic pyrolysis of random PP produced gasoline- and diesel-range hydrocarbons.

Keywords: SAPO-11, catalytic pyrolysis, miscanthus, random polypropylene.

Introduction

With the increasing demand for renewable energy, lignocellulosic biomass has attracted considerable attention. Lignocellulosic biomass consists mainly of three bio-polymers: cellulose, hemicellulose and lignin. Lignocellulosic biomass can be converted to energy using thermal conversion technologies, which can be divided into combustion, gasification and pyrolysis. Fast pyrolysis is aimed at maximizing the production of bio-oil at very high heating rates under oxygen-free

conditions. The bio-oil produced from fast pyrolysis, however, has several drawbacks, such as low heating value and high oxygen and water contents, which require further upgrading. Atmospheric-pressure catalytic pyrolysis is considered an effective technique that can improve the bio-oil quality by removing oxygen from bio-oil into gaseous species, such as CO, CO₂ and H₂O.¹⁻⁴

Among a range of lignocellulosic biomass materials, miscanthus is considered one of the representative energy crops owing to the ease of cultivation and harvest, high yield and high heating value.^{5,6} Recently, the production of bio-oil from the pyrolysis of miscanthus has attracted considerable research attention but the bio-oil derived from miscanthus also requires

†To whom correspondence should be addressed.
E-mail: catalica@uos.ac.kr

adequate catalytic upgrading to improve its quality.⁷ The catalytic pyrolysis of miscanthus, however, has received less attention than that of other biomass materials. Zeolite-based or mesoporous catalysts are commonly used for the catalytic pyrolysis of miscanthus.

The recycling of municipal solid waste is another important issue in terms of the effective use of limited energy resources. In particular, the recycling of waste plastics, such as polyethylene and polypropylene has attracted considerable attention.⁸ Because plastic materials are not bio-degradable, they need to be treated using suitable techniques. Fuel oil can be produced from the pyrolysis of plastics but its quality is normally low, and high temperatures are required to obtain a high oil yield. On the other hand, the catalytic pyrolysis of plastics can produce bio-oil with higher quality containing gasoline- or diesel-range hydrocarbons, while lowering the reaction temperature.^{8,9} The catalysts normally used for the catalytic pyrolysis of plastics are also zeolite-based catalysts, such as HZSM-5 and HY, or mesoporous catalysts, such as MCM-41, MCM-48, and SBA-16.

Silicoaluminophosphate (SAPO) catalysts have been applied successfully to a range of industrial processes including methanol-to-olefin, isomerization and cracking reactions but they have seldom been applied to the pyrolysis of biomass. Despite its high potential for the catalytic pyrolysis of polymer materials, SAPO-11 has never been applied to the pyrolysis of biomass or random polypropylene (random PP). Therefore, the applications of SAPO-11 to the pyrolysis of bio-polymers and waste plastics, such as miscanthus and random PP, needs to be studied to extend the applicability of the SAPO catalysts and seek an effective way to upgrade bio-oil.

In this study, SAPO-11 was applied to the pyrolysis of miscanthus and random PP, which are typical bio-polymer materials and waste plastics, respectively. The effects of the catalytic properties of SAPO-11 on the pyrolysis product distribution were investigated.

Experimental

Miscanthus and Random PP. Random PP (Samsung Total) and wild miscanthus, which grows naturally in Korea, were used in the experiments. Table 1 lists the proximate analysis results for the random PP and wild miscanthus used in this study. The moisture, volatiles and ash contents were measured based on the ASTM D2016-74, ASTM E897-82, and ASTM D1102-84 standards, respectively. The miscanthus (2.4 mg)

Table 1. Proximate Analysis Results of Miscanthus and Random PP

Proximate analysis	Miscanthus (wt%)	Random PP (wt%)
Moisture	1.21	0.61
Volatiles	78.6	98.72
Fixed carbon	13.8	0.44
Ash	6.39	0.23

and random PP (8 mg) samples were used for proximate analysis. To determine the moisture content, each sample was heated from room temperature to 110 °C, and the temperature was maintained at 110 °C for 1 h. The volatile content was determined by heating the sample to 900 °C and measuring the mass reduction. The temperature was then decreased to 800 °C and maintained at that temperature in an oxygen atmosphere until no further mass change was observed. The difference between the original mass and the remaining mass was considered to be the fixed carbon content; the remaining mass was regarded as the ash content.¹⁰

Preparation of Catalysts. SAPO-11 catalyst was purchased from Tianjin Chemist Scientific Ltd.

Characterization of Catalysts. The BET surface area was determined by N₂ adsorption at -196 °C using a Micromeritics ASAP 2010. The structure of the catalyst was examined by powder X-ray diffraction (XRD, Rigaku D/max-2500) using Cu K α radiation ($\lambda=15406$ nm). NH₃-temperature programmed desorption was performed in a 40 mL/min helium flow to determine the acidity of the catalyst. Ammonia was adsorbed at 100 °C.¹¹ The desorption process was monitored with a TCD while the temperature was ramped from 100 to 600 °C with a rate of 20 °C/min.

The nature of the acid sites was examined using pyridine as a probe molecule. 0.26 g of self-supported wafer samples with a diameter of 13 mm was prepared by applying a pressure of 3 tons. The samples were placed in the sample holder under vacuum conditions and temperature was maintained at 350 °C for 1 h. The samples were then cooled to room temperature and exposed to a pyridine vapor flow with a set dose until the catalyst surface was saturated. Pyridine was then desorbed until the pressure reached 10⁻³ Torr to ensure that no physisorbed pyridine was present on the sample. Fourier transform infrared (FTIR, Spectrum GX Perkin Elmer) spectroscopy was performed using a mercury-cadmium-telluride detector. The wafers containing the chemisorbed pyridine were subjected to a thermal treatment at 150 or 300 °C and the FTIR spectra

were recorded *in situ*.

Thermogravimetric Analysis (TGA). Thermogravimetric analysis of the samples (miscanthus and random PP) was performed using a thermogravimetric analyzer (Perkin Elmer, Pyris 1). 2 mg of miscanthus and 3.5 mg of random PP were used for analysis. The heating rate was 30 °C/min. Two mass ratios between the catalyst and sample were used: 1:1 and 1:2. Three different heating rates, 20, 30 and 40 °C/min, were used to determine the activation energy. The reader can refer to a previous study¹⁰ for more detailed information.

Py-GC/MS Analysis. Py-GC/MS was used to examine the pyrolysis product distribution. A vertical furnace type pyrolyzer (py-2020D, Frontier-Lab Co.) was used. Non-catalytic pyrolysis experiments were carried out using 1.5 mg of miscanthus and 1 mg of random PP. In the catalytic pyrolysis experiments, each sample was placed into a metal sample cup, an intermediate layer was made with quartz wool over the sample layer, and the catalyst was placed over the quartz wool layer. The sample/catalyst ratio was set to 1/1 and 1/2 to examine the effect of the catalyst dose. The reaction temperature was set to 550 °C. The product vapor was trapped by Microjet Cryo-Trap (MJT 1030E) and after 3 min was analyzed by gas chromatography (GC, HP 7890A)/mass spectrometry (MS, HP 5975 inert Mass Spectral Detector) connected directly to the pyrolyzer. The metal capillary column used for GC/MS analysis was Ultra ALLOY-5 (MS/HT) (5% diphenyl and 95% dimethylpolysiloxane, length 30 m, i.d. 0.25 mm, film thickness 0.5 µm, Frontier Laboratories Ltd. Japan). He carrier gas with a split ratio of 50:1 was used. The GC oven was heated from 40 to 300 °C at a rate of 5 °C/min. Each peak was analyzed using the NIST05 library. Area% was used for analysis.

Results and Discussion

Characterization of Catalyst. The BET surface area and total pore volume (V_{total}) of SAPO-11 obtained using the nitrogen sorption method were 121 m²/g and 0.15 cm³/g, respectively. Figure 1 shows a typical XRD pattern of SAPO-11.

Figure 2 shows the NH₃-TPD analysis result. The peak at 160 °C indicates weak acid sites, whereas that at 240 °C represents medium-strength acid sites. Figure 3 shows the pyridine FTIR result. The desorption curve for 150 °C suggests that SAPO-11 possesses two types of acid sites, i.e. Lewis acid sites represented by the peak appearing at 1450 cm⁻¹ and Brønsted acid sites represented by the peak appearing at 1540 cm⁻¹. On the other hand, in the desorption curve for 300 °C, most

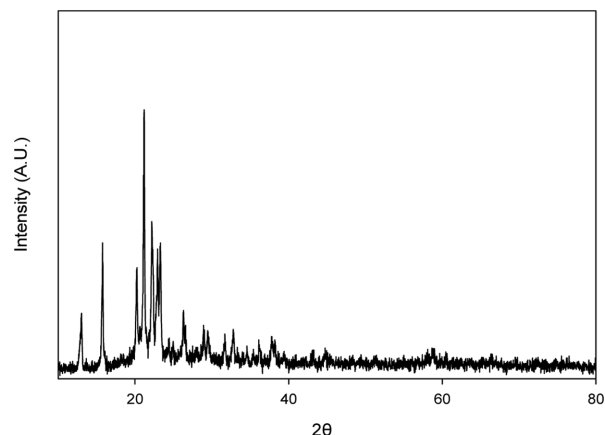


Figure 1. XRD pattern of SAPO-11.

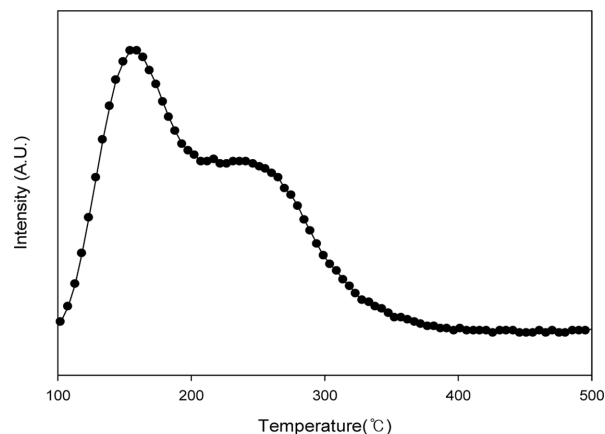


Figure 2. NH₃-TPD of SAPO-11.

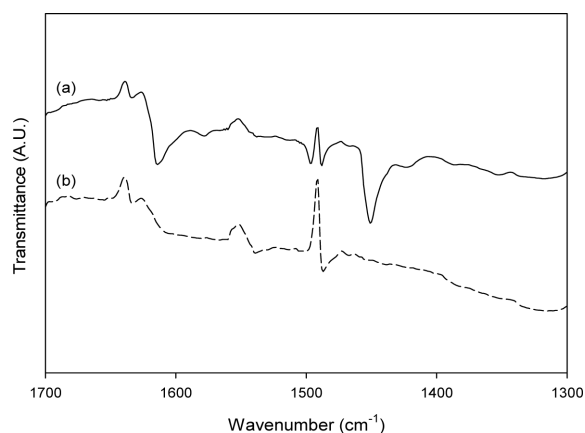


Figure 3. Pyridine FTIR of SAPO-11. Desorption of adsorbed pyridine at (a) 150 °C; (b) 300 °C.

Lewis acid sites had disappeared, whereas the peak representing Brønsted acid sites at 1540 cm⁻¹ was still observed. This suggests that the weak and medium-strength acid sites observed in the NH₃-TPD (Figure 2) are mainly Lewis and

Brønsted acid sites, respectively. Overall, SAPO-11 has two types of acid sites with sufficient levels, suggesting the feasibility of the catalytic pyrolysis of miscanthus and random PP over SAPO-11.

TGA. Figure 4 shows the TGA results of miscanthus and random PP. In the non-catalytic pyrolysis of miscanthus (Figure 4(a)), the evaporation of moisture began at approximately 100 °C. The pyrolysis reaction was initiated at approximately 200 °C and was almost complete at approximately 400 °C with the remaining mass being char. The mass reduction observed at 200~350 °C was attributed to the decomposition of hemicellulose,^{10,12} whereas the mass reduction observed at 350~380 °C was due to the decomposition of cellulose.^{10,12} Compared to the regular crystal-shaped linkage between cellulose polymers, the linkage between hemicellulose polymers is weak because hemicellulose is a heterogeneous polysaccharide. Lignin begins to decompose slowly over a wide temperature range of 200~600 °C because it is a polymer with a complex structure requiring high temperatures for complete decomposition.

The decomposition temperature of miscanthus in catalytic pyrolysis was similar to that in non-catalytic pyrolysis, probably because the molecular structure of miscanthus is too large to enter the pores of SAPO-11. Nevertheless, the mass reduction of miscanthus was more profound in catalytic pyrolysis than in the non-catalytic pyrolysis. When the mass ratio between SAPO-11 and miscanthus was 1:1, moisture evaporation at approximately 100 °C increased slightly, and the amount of final residue (char) was decreased by the catalyst. When the mass ratio between SAPO-11 and miscanthus was changed to 2:1, the initial dehydration increased and the char yield decreased. This might be due to the increased accessibility of the miscanthus sample to the external surface of the SAPO-11 catalyst. Increasing the level of catalyst appeared to inhibit secondary reactions, e.g., polymerization, of pyrolysis product vapors, resulting in the suppression of char formation and enhanced conversion to oil and gas. Luo *et al.*¹³ performed the catalytic pyrolysis of lignin over several catalysts, such as USY, HZSM-5 and H β , using TG-FTIR and reported that dehydration was promoted and char formation was suppressed by the catalysts, which is in agreement with these results.

Figure 4(b) shows that in the case of the catalytic pyrolysis of random PP, decomposition took place at approximately 400 °C, which is lower than the decomposition temperature range of the non-catalytic pyrolysis (400~500 °C). In the presence of a catalyst, the molten random PP entered the pores of the catalyst and is decomposed more easily by the acid sites.

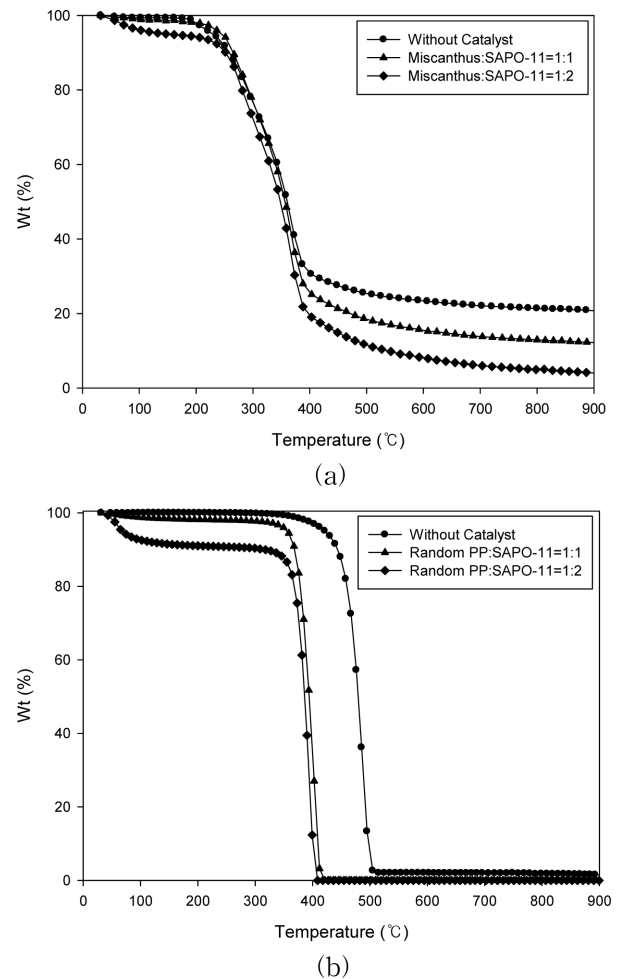


Figure 4. TG curves of (a) miscanthus; (b) random PP.

On the other hand, when the polymer/catalyst ratio was changed from 1:1 to 1:2, the decrease in decomposition temperature was marginal. This suggests that the catalyst dose corresponding to a 1:1 polymer/catalyst ratio is sufficient to guarantee contact between the random PP and catalyst.

TGA is used widely to examine the thermal characteristics of polymers, and has been used to estimate the activation energy. The TG graph is determined by thermodynamic variables, such as the activation energy, Arrhenius frequency factor and reaction order.

For the reaction $aX_{(s)} + bB_{(g)} \rightarrow cC_{(s)} + dD_{(g)}$, the reaction rate can be expressed by

$$\frac{dX}{dt} = kf(X) \quad (1)$$

The reaction rate constant k is given by the Arrhenius equation as follows:

Table 2. Activation Energy Determined at Different Levels of Conversion X

Miscanthus		Random PP		Random PP/SAPO-11 (1/1)		Random PP/SAPO-11 (1/2)	
Conversion, X	Activation energy [kJ/mol]	Conversion, X	Activation energy [kJ/mol]	Conversion, X	Activation energy [kJ/mol]	Conversion, X	Activation energy [kJ/mol]
0.1	151.41	0.1	203.22	0.1	129.83	0.1	90.20
0.2	160.91	0.2	214.16	0.2	112.79	0.2	141.48
0.3	200.07	0.3	211.91	0.3	112.69	0.3	125.49
0.4	188.94	0.4	184.93	0.4	103.62	0.4	107.03
0.5	220.93	0.5	212.80	0.5	109.98	0.5	117.25
0.6	213.31	0.6	193.90	0.6	118.29	0.6	122.38
0.7	200.62	0.7	219.63	0.7	112.90	0.7	111.94
0.8	235.07	0.8	215.81	0.8	161.98	0.8	112.91
Average	196.4	Average	207.0	Average	120.3	Average	116.1

$$k = A \exp\left(\frac{-E}{RT}\right) \quad (2)$$

where, A is the Arrhenius frequency factor, R is the gas constant, T is temperature, and E is the activation energy. $f(X)$ is a function of conversion expressed as follows:

$$f(X) = (1-X)^n \quad (3)$$

Several methods can be used to determine the activation energy based on the above-shown equations.¹⁰ In this study, the Friedman method, which is an iso-conversional method, was used to determine the activation energy. eq. (4) can be derived by substituting eqs. (2) and (3) into eq. (1) and taking the natural logarithms on both sides:

$$\ln\left(\frac{dX}{dt}\right) = \ln A + n \ln(1-X) - \frac{E}{RT} \quad (4)$$

Based on this equation, the activation energy E can be obtained by plotting $\ln(dX/dt)$ vs. $1/T$.

Table 2 lists the activation energy determined at different levels of conversion, X . In the absence of a catalyst, the mean activation energy of miscanthus was 196.4 kJ/mol (range 150~236 kJ/mol), whereas that of random PP was 207.1 kJ/mol (range 184~220 kJ/mol). In the case of catalytic pyrolysis of random PP over SAPO-11, the activation energy was 120.3 kJ/mol (range 103~162 kJ/mol) and 116.1 kJ/mol (range 90~142 kJ/mol) when the polymer/catalyst ratio was 1:1 and 1:2, respectively. Doubling the catalyst ratio did not affect the activation energy significantly. As mentioned above, a polymer/catalyst ratio of 1:1 is sufficient to guarantee contact between random PP and catalyst. Park *et al.*,^{8,9} in their study of the catalytic pyrolysis of polymers, over ferrierite, MCM-48,

and SBA-16, also reported that the activation energy was reduced by the presence of a catalyst.

Catalytic Pyrolysis. Figure 5 shows the product distribution obtained from the pyrolysis of miscanthus over SAPO-11. The pyrolysis product species were grouped into six categories: acids, hydrocarbons, oxygenates, phenolics, aromatics and PAHs. All acids appeared to be acetic acids. Oxygenates were the dominant products of non-catalytic pyrolysis. In the presence of a catalyst, however, the production of oxygenates was reduced substantially, whereas the production of acids, hydrocarbons, phenolics, aromatics and PAHs was increased. The reduced production of oxygenates is encouraging because they deteriorate the quality of bio-oil. Antonakou *et al.*¹⁴ and Adam *et al.*¹⁵ performed the catalytic pyrolysis of commercial wood and miscanthus, and reported that the use of a catalyst increased the phenolics yield, while reducing the oxygenate

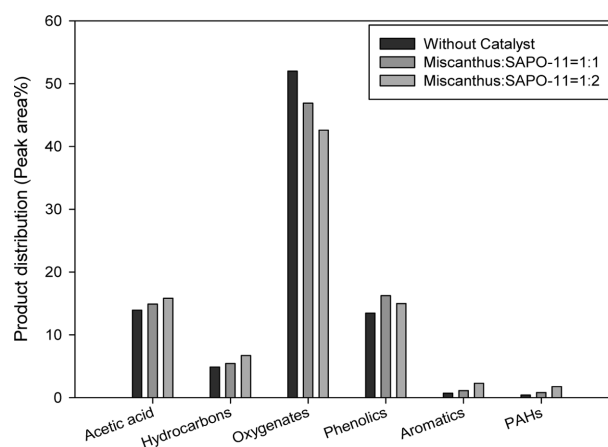


Figure 5. Product distribution from pyrolysis of miscanthus over SAPO-11.

yield.

When the catalyst dose was doubled (Figure 5), the oxygenate yield decreased further, whereas the yields of acids, hydrocarbons, aromatics and PAHs increased further. The phenolic yield, however, decreased when the catalyst concentration was doubled, probably because some phenolics species were converted to aromatics. From their experiments on the catalytic pyrolysis of lignin, Lee *et al.*¹⁶ reported that the increased catalyst dose resulted in a decreased phenolic yield due to the enhanced conversion of phenolics to aromatics, which is in good agreement with the results of the present study.

The increased acid yield with increasing catalyst concentration is a potential problem because the acidity of bio-oil can cause the corrosion of combustors. Therefore, an additional separation process may be needed.

Figure 6 compares the detailed oxygenate species distribution obtained with different catalyst doses. In the absence of a catalyst, ketones, furans, levoglucosan and cyclocompounds were main oxygenate products. With increasing catalyst concentration, the fractions of levoglucosan and ketones decreased, whereas those of furans and cyclocompounds increased. Carbohydrates, such as levoglucosan are converted to furans in the presence of an acid catalyst, such as SAPO-11, due to an enhanced dehydration reaction.¹⁷ The furan yield was highest when the biomass/catalyst ratio was 1:1. The furan yield decreased when the catalyst dose was doubled, possibly due to the enhanced conversion of furans to aromatics. Park *et al.*¹⁸ reported that an increase in the Meso-Y catalyst dose resulted in a decrease in furan yield and an increase in the aromatic

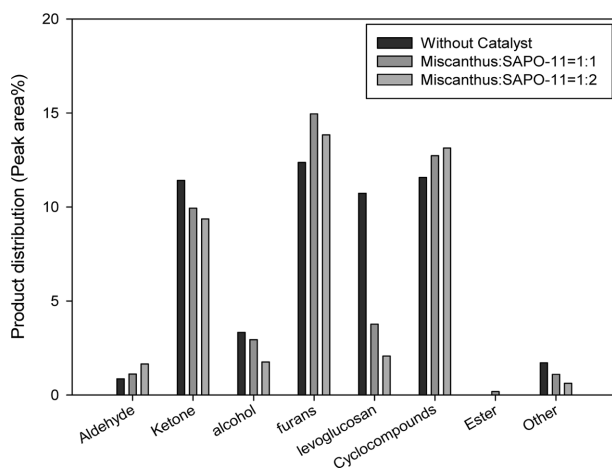


Figure 6. Effects of catalyst on the oxygenate distribution for the pyrolysis of miscanthus over SAPO-11.

yield in the pyrolysis of cellulose. Cheng and Huber¹⁹ also reported the conversion of furans to aromatics in the presence of acid catalysts. The decrease in the alcohol yield is also believed to be due to their conversion to aromatics.

Detailed analysis of furans (data not shown) showed that the formation of low-molecular-mass furans, such as furfural and 2,3-dihydrofuran, increased with increasing catalyst concentration, whereas that of high-molecular-mass furans, such as 2,3-dihydrobenzofuran, decreased. This was attributed to the enhanced cracking by SAPO-11. Jeon *et al.*¹⁷ who examined the catalytic pyrolysis of cellulose, also reported that high-molecular-mass furans were converted to low-molecular-mass furans under increasing Al-SBA-15 catalyst dose. Because furans, particularly low-molecular-mass furans (e.g. furfural), are important materials used as building block materials in the petroleum chemical industry, the enhanced production of these species is beneficial for bio-oil quality improvement.

Phenolics produced from pyrolysis processes are important basic raw materials in the petroleum chemical industry. They can be used not only as building block materials for phenolic resin, but also as natural antioxidants.^{20,21} Therefore, an increased phenolic yield is a positive result in the catalytic upgrading of bio-oil. The employment of SAPO-11 catalyst increased the phenolic yield compared to non-catalytic pyrolysis. Doubling the catalyst dose, however, decreased the phenolic yield slightly. A previous study reported that phenolics are converted to aromatics in the presence of a sufficient quantity of acid sites.¹⁶ Detailed analysis of the phenolic species (data not shown) showed that the presence of a catalyst promoted the formation of light phenolics, such as phenol and ethyl phenol, while reducing the production of heavy phenolics. This was attributed to the enhanced cracking of heavy phenols derived from lignin to light phenols in the presence of an acid catalyst. Doubling the catalyst dose increased the yield of light phenolics even further (data not shown).

Figure 7 shows the aromatic species distributions obtained with different catalyst doses. In the non-catalytic pyrolysis, only a small quantity of benzene and toluene were produced. On the other hand, the use of SAPO-11 as a catalyst increased the yields of these two species and produced another species, o-xylene. Doubling the catalyst dose enhanced the production of these three aromatic species further. Because BTEX (benzene, toluene, ethylbenzene and xylene) species are important raw materials in the chemical industry, increasing the aromatic yield is important for increasing the value of bio-oils. The production of aromatics is accomplished by chemical reactions

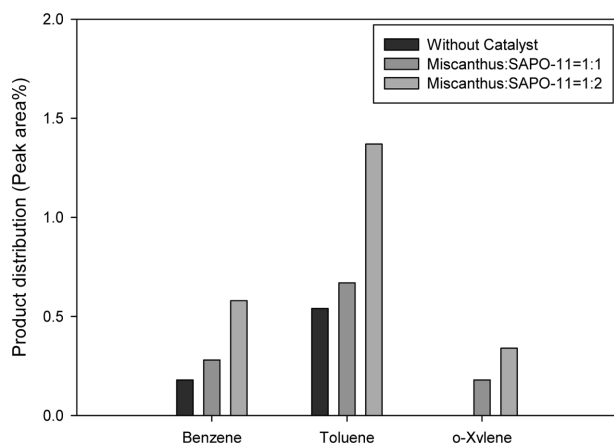


Figure 7. Effects of catalyst on the aromatic products from the pyrolysis of miscanthus over SAPO-11.

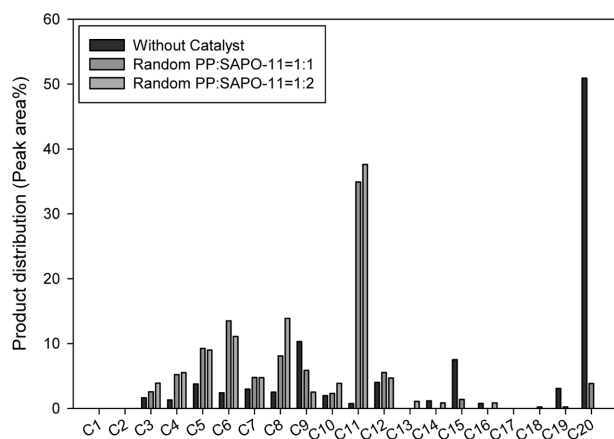


Figure 8. Product distribution of random PP over SAPO-11.

that take place in the presence of acid sites, such as cracking, oligomerization, dehydrogenation and aromatization. Therefore, the increased aromatic yield with increasing catalyst concentration can be attributed to larger number of acid sites.

The products of the pyrolysis of random PP over SAPO-11 were divided based on their carbon numbers (Figure 8). When random PP was pyrolyzed without a catalyst, wax-like polymers with a carbon number of 20 or larger were mainly produced. Catalytic cracking of these polymers into lighter molecules can increase the value of the resulting bio-oil. Catalytic upgrading increased substantially the yields of light species with carbon numbers of 12 or less. When the polymer/catalyst ratio was 1/1, diesel-range species, e.g., C11, and gasoline-range species (C5~C9) were the main products, which means that the value of the product was increased significantly by catalytic upgrading. Doubling the catalyst dose did not affect the carbon number distribution significantly.

Conclusions

Miscanthus, a representative biopolymer, and random PP, a representative plastic, were pyrolyzed over SAPO-11 catalyst. SAPO-11 contains both weak and medium-strength acid sites. For both miscanthus and random PP, the product of catalytic pyrolysis contained more valuable species than that of non-catalytic pyrolysis. TGA showed that SAPO-11 induced dehydration and suppressed char formation in the pyrolysis of miscanthus and reduced the decomposition temperature of random PP. The mean activation energy for the decomposition of miscanthus and random PP was 196.4 and 207.1 kJ/mol, respectively. The mean activation energy of random PP was reduced by SAPO-11. The yield of oxygenates, which deteriorate the quality of bio-oil, from the catalytic pyrolysis of miscanthus was much smaller than that obtained from non-catalytic pyrolysis, whereas the yield of phenolics, furans and aromatics were increased by the catalyst, showing improved bio-oil quality. Doubling the catalyst dose decreased the yield of phenolics and furans, while increasing the aromatic yield, indicating the conversion of phenolics and furans to aromatics. The carbon number of the main products of the non-catalytic pyrolysis of random PP was more than 20. When catalytic pyrolysis was performed over SAPO-11, however, the main product was C11, which is a diesel-range product. In addition, gasoline-range products (C5~C9) were produced.

Acknowledgement: This work was supported by the 2011 Research Fund of the University of Seoul.

References

1. C. H. Ko, S. H. Park, J. K. Jeon, D. J. Suh, K. E. Jeong, and Y. K. Park, *Korean J. Chem. Eng.*, **29**, 1657 (2012).
2. H. J. Park, J. K. Jeon, D. J. Suh, Y. W. Suh, H. S. Heo, and Y. K. Park, *Catal. Surv. Asia*, **15**, 161 (2011).
3. M. J. Jeon, S. J. Choi, K. S. Yoo, C. Ryu, S. H. Park, J. M. Lee, J. K. Jeon, Y. K. Park, and S. Kim, *Korean J. Chem. Eng.*, **28**, 497 (2011).
4. H. J. Park, H. S. Heo, K. S. Yoo, J. H. Yim, J. M. Sohn, K. E. Jeong, J. K. Jeon, and Y. K. Park, *J. Ind. Eng. Chem.*, **17**, 549 (2011).
5. H. S. Heo, H. J. Park, J. H. Yim, J. M. Sohn, J. Park, S. S. Kim, C. Ryu, J. K. Jeon, and Y. K. Park, *Bioresour. Technol.*, **101**, 3672 (2010).
6. A. Sørensen, P. J. Teller, T. Hilstrøm, and B. K. Ahring, *Bioresour. Technol.*, **99**, 6602 (2008).
7. H. J. Park, K. H. Park, J. K. Jeon, J. N. Kim, R. Ryoo, K. E. Jeong, S. H. Park, and Y. K. Park, *Fuel*, **97**, 379 (2012).

8. S. J. Choi, Y. K. Park, K. E. Jeong, T. W. Kim, H. J. Chae, S. H. Park, J. K. Jeon, and S. S. Kim, *Korean J. Chem. Eng.*, **27**, 1446 (2010).
9. H. J. Park, Y. K. Park, J. I. Dong, J. K. Jeon, J. H. Yim, and K. E. Jeong, *Res. Chem. Intermed.*, **34**, 727 (2008).
10. J. W. Kim, S. H. Lee, S. S. Kim, S. H. Park, J. K. Jeon, and Y. K. Park, *Korean J. Chem. Eng.*, **28**, 1867 (2011).
11. Y. K. Park, S. J. Kim, C. N. You, J. Cho, S. J. Lee, J. H. Lee, and J. K. Jeon, *J. Ind. Eng. Chem.*, **17** 186 (2011).
12. Y. M. Kim, H. W. Lee, S. H. Lee, S. S. Kim, S. H. Park, J. K. Jeon, S. Kim, and Y. K. Park, *Korean J. Chem. Eng.*, **28**, 2012 (2011).
13. Z. Luo, S. Wang, and X. Guo, *J. Anal. Appl. Pyrolysis*, **95**, 112 (2012).
14. E. Antonakou, A. Lappas, M. H. Nilsen, A. Bouzga, and M. Stöcker, *Fuel*, **85**, 2202 (2006).
15. J. Adam, E. Antonakou, A. Lappas, M. Stöcker, M. H. Nilsen, A. Bouzga, J. E. Hustad, and G. Øye, *Micropor. Mesopor. Mater.*, **96**, 93 (2006).
16. H. W. Lee, T. W. Kim, S. H. Park, J. K. Jeon, D. J. Suh, and Y. K. Park, *J. Nanosci. Nanotechnol.*, **13**, 2640 (2013).
17. M. J. Jeon, J. K. Jeon, D. J. Suh, S. H. Park, Y. J. Sa, S. H. Joo, and Y. K. Park, *Catal. Today*, **204**, 170 (2013).
18. Y. K. Park, B. R. Jeon, S. H. Park, J. K. Jeon, D. J. Suh, S. S. Kim, and K. E. Jeong, *J. Nanosci. Nanotechnol.*, Accepted.
19. Y. T. Cheng and G. W. Huber, *ACS Catal.*, **1**, 611 (2011).
20. S. Tsubaki, M. Sakamoto, and J. I. Azuma, *Food Chem.*, **123**, 1255 (2010).
21. K. Murata, Y. Liu, M. Inaba, and I. Takahara, *J. Anal. Appl. Pyrolysis*, **94**, 75 (2012).